ARTICLES

Photochromism of WO_3 Colloids Combined with TiO_2 Nanoparticles

Tao He, Ying Ma, Yaan Cao, Xiaoliang Hu, Haimei Liu, Guangjin Zhang, Wensheng Yang, and Jiannian Yao*

Center for Molecular Sciences & Institute of Chemistry, Chinese Academy of Sciences, Beijing 100080, People's Republic of China

Received: April 28, 2002

WO_3 and TiO_2 colloids were synthesized by the forced hydrolysis technique, and different amounts of the TiO_2 colloids were added to WO_3 colloids under sonication to get stable combined TiO_2 and WO_3 colloids (WO_3/TiO_2). The experimental results indicate that the UV-light coloration of WO_3 colloids can be improved greatly after the TiO_2 combination. When the molar ratio of TiO_2 and WO_3 is about 1:40, ΔOD at 900 nm for WO_3/TiO_2 colloids is about 12.7 times that of WO_3 colloids. The improvement effect increases with the increased concentration of TiO_2 in the composite colloids, and the maximum enhancement can increase more than 50-fold. It is shown that after the combination, the recombination of photogenerated carriers is suppressed efficiently, and more electrons can be trapped within the band gap of WO_3 to contribute to the coloration process.

1. Introduction

During the past two decades, investigations of colloidal semiconductor suspensions have become quite popular because of their interesting photophysical and photochemical processes.[1−11] Among the semiconductors, WO_3 has received considerable attention because of its photo- and electrochromic properties.[6−22] Since the photochromic process of WO_3 can be made completely reversible by exposing it to oxygen,[12,13] it has been considered to be one of the most promising candidates for technological applications such as erasable optical storage devices and large-area displays. The UV-light photochromism of WO_3 may be improved by suppressing the recombination process of photogenerated carriers since their efficient utilization dictates this coloration process. For example, gold nanoparticles can enhance the UV-light coloration behavior of WO_3 thin films by suppressing the recombination process through a Schottky barrier formed at the interface of gold and WO_3 films.[22] If WO_3 is combined with a photoresponsive semiconductor material with a different energy-band structure, then its optical properties are also expected to be improved by the enhanced charge-carrier separation.[1]

TiO_2 is an attractive material with excellent photoresponsive properties, and some researchers have attempted to improve the coloration performance of WO_3 by TiO_2.[23,24] However, it is still unclear how TiO_2 influence the photochromism of WO_3. In our work, $H_2C_2O_4$ was used as a peptizing agent in the preparation of WO_3 colloids, which can also act as efficient hole scavengers to improve the photochromism of WO_3. It is found after the combination of TiO_2 that the detrimental recombination of photogenerated carriers is suppressed efficiently and that there are more electrons trapped within the band gap of WO_3 contributing to the coloration process. On the basis of the fluorescence spectral results and energy-band theory, a diagram of the energy levels of the WO_3/TiO_2 system is proposed to explain the enhancement effects of TiO_2.

2. Materials and Methods

Materials. Sodium tungstate ($Na_2WO_4 \cdot 2H_2O$), oxalic acid ($H_2C_2O_4 \cdot 2H_2O$), and titanium tetrabutoxide ($Ti(OC_4H_9)_4$) were purchased from Beijing Chemical Company (analytic reagent grade). All other reagents were analytic reagent grade and were used as received without further purification. The water used in all experiments was high-purity water (18.2 MΩ cm).

Preparation of the Colloids. TiO_2 colloids were prepared in light of refs 5 and 25. Titanium tetrabutoxide was used as the precursor, and anhydrous ethanol, as the solvent. The reaction was carried out at room temperature with vigorous stirring. The concentration of TiO_2 in the sol that was obtained was about 0.26 mol/L.

A series of transparent colloidal suspensions of WO_3 were prepared by the method described previously.[6,10] In a typical preparation procedure, 6.6 g of $Na_2WO_4 \cdot 2H_2O$ was dissolved in 100 mL of water. After the solution was bubbled with Ar for ca. 15 min, concentrated HCl was added dropwise into the solution without stirring until the pH of the system reached ca. 3.0. The white, gelatinous precipitate that was obtained was washed several times by decantation at ca. 0 °C under an Ar atmosphere. The precipitate was then dissolved in a hot $H_2C_2O_4$ solution (3.8 g in 30 mL water) under sonication, and the suspension was then diluted to 100 mL. The pH of the original colloids was less than 1.0. The concentration of WO_3 was in the range from 0.05 to 0.4 mol/L, whereas the concentration of $H_2C_2O_4$ was fixed at 0.3 mol/L. $H_2C_2O_4$ could be removed from the suspension by dialyzing against H_2SO_4 solution. After the

* Corresponding author. E-mail: jnyao@infoc3.icas.ac.cn. Tel: +86-10-8261-6517. Fax: +86-10-6487-9375.

10.1021/jp026031t CCC: $22.00
Published on Web 11/16/2002

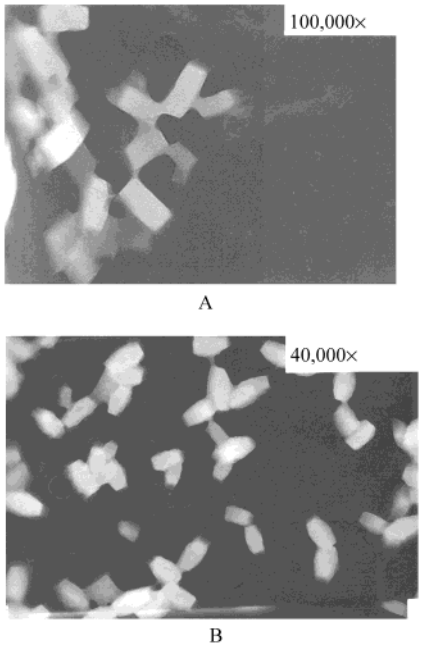

Figure 1. TEM images of WO_3 colloids. The concentrations of WO_3 are ca. (A) 0.1 and (B) 0.2 mol/L.

addition of TiO_2, WO_3 colloids combined with TiO_2 nanoparticles were obtained after sonication. In this work, unless otherwise stated, the concentration of WO_3 in WO_3 and WO_3/TiO_2 colloids is ca. 0.2 mol/L, and that of TiO_2 in the WO_3/TiO_2 colloids is ca. 5.1 mmol/L.

Measurements. For the transmission electron microscopy examination of the colloids, a small drop of the suspension was applied to carbon-coated copper grids. A JEOL 2000EX transmission electron microscope (TEM) was used to observe the morphology and determine the particle sizes. The UV-light coloration was carried out by irradiating the colloids with the UV output of a 500-W high-pressure mercury lamp. The UV−vis absorption spectra were measured by using a Shimadzu UV-1601PC double-beam UV−vis spectrophotometer. The steady-state fluorescence spectra were recorded with a Hitachi F-4500 spectrometer. The surface photovoltage spectroscopy (SPS) measurements were performed on a homemade instrument,[26,27] from which the spectra were normalized because of the different intensity distribution of the light source. Raman spectra were recorded on a Renishaw 2000 spectrometer with the Ar^+ line (514.5 nm) as the excitation source.

3. Results

Characterization of the Colloids. A series of transparent WO_3 colloids with different concentrations were prepared; these were stable for several months at room temperature. The diameter of the nanoparticles is in the range of several to tens of nanometers, which increases with the increased concentration of WO_3. Some of the TEM images, which indicate that the shape of the WO_3 particles is regularly rectangular, are shown in Figure 1. Figure 2 gives the TEM image of a spherical TiO_2 particle, and its average diameter is about 5 nm. After the combination of WO_3 and TiO_2, the size of the composite particles is larger than that of WO_3 or TiO_2 particles, and the shape of the particles changes slightly, as shown in the TEM images (Figure 3). Since the flat-band potentials (E_{fb}) of WO_3 and TiO_2 colloids are 0.33 and −0.2 V, respectively, in the acid system,[6,7] the charges on these two colloids should be opposite. Therefore, it is reasonable for the WO_3 and TiO_2 colloids to undergo aggregation due to the electrostatic force when they are mixed together, leading to good contact between TiO_2 and WO_3 particles. When the amount of TiO_2 is higher than 30 mol %, the colloids will become unstable and begin to precipitate. According to the UV−vis spectra of virgin WO_3, TiO_2, and WO_3/TiO_2 colloids (Figure 4), the absorption edge shifts to a longer wavelength (red shift) in the case of WO_3/TiO_2 colloids,

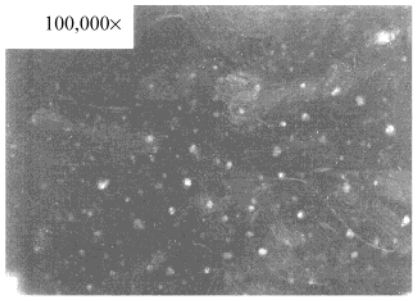

Figure 2. TEM image of the TiO_2 colloid.

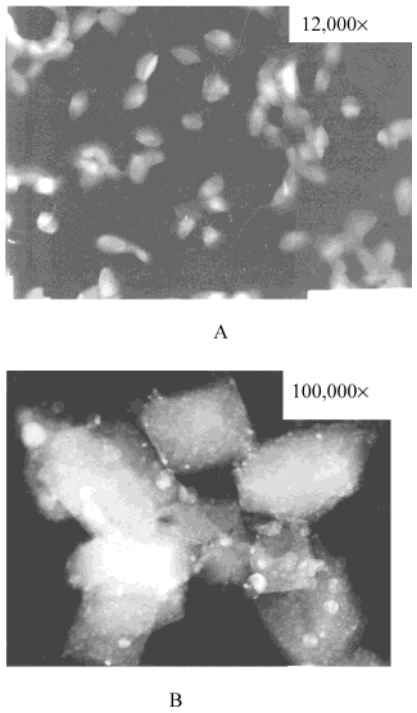

Figure 3. TEM images of WO_3/TiO_2 colloids. The concentrations of WO_3 and TiO_2 are ca. 0.1 mol/L and 5.1 mmol/L, respectively.

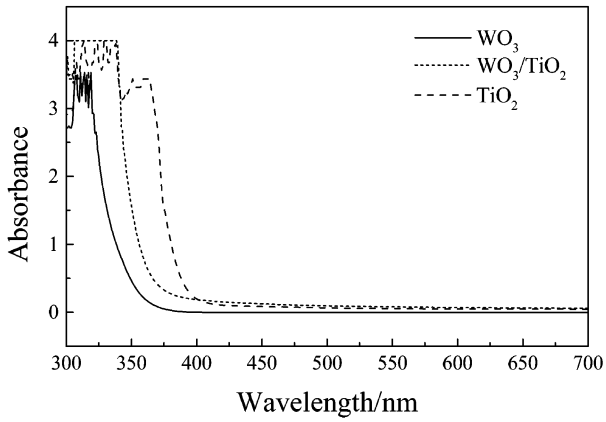

Figure 4. UV−vis spectra of virgin WO_3, TiO_2, and WO_3/TiO_2 colloids.

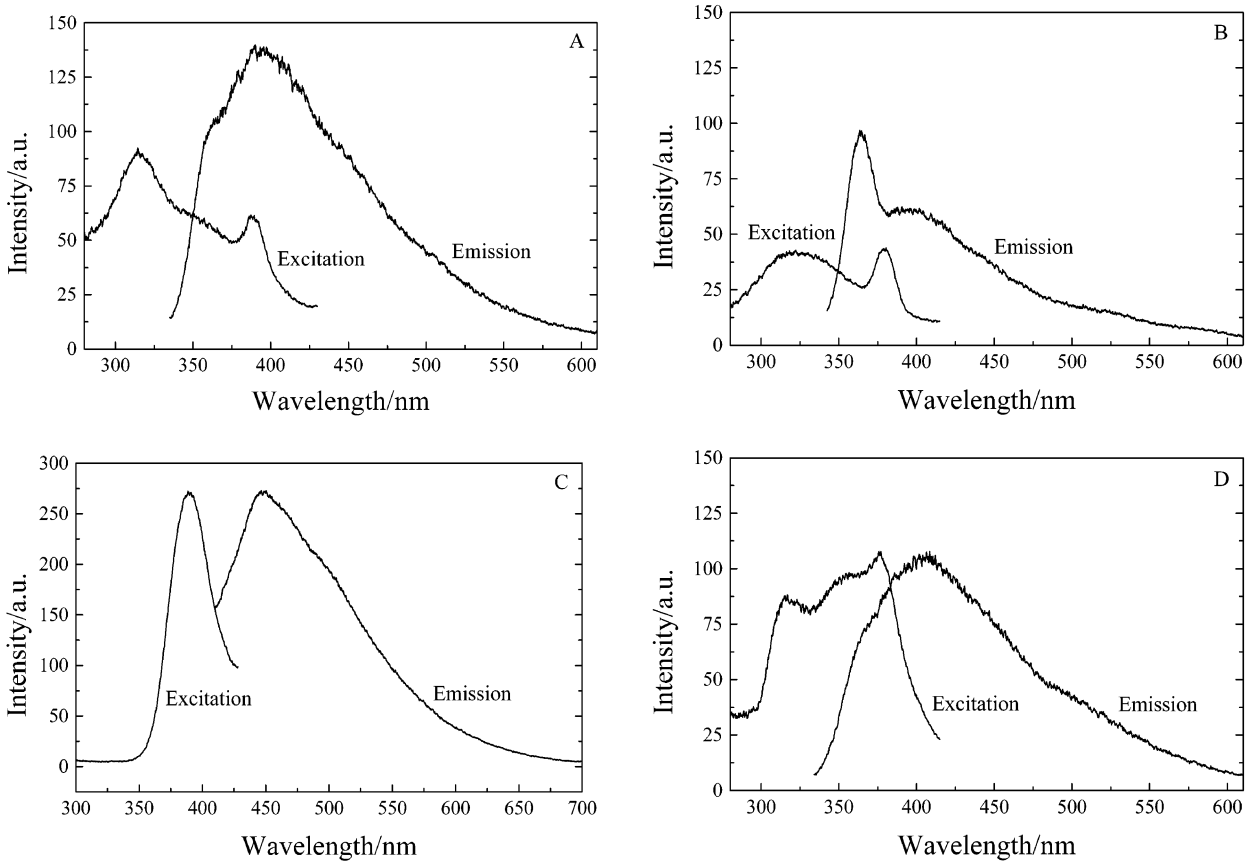

Figure 5. Emission and excitation spectra of WO_3 (A) with and (B) without $H_2C_2O_4$, (C) TiO_2, and (D) WO_3/TiO_2 colloids. The emission spectra were collected at excitation wavelengths of 315 (A, B, and D) and 395 nm (C). The excitation spectra were acquired at an emission wavelength of 440 nm for all of the samples.

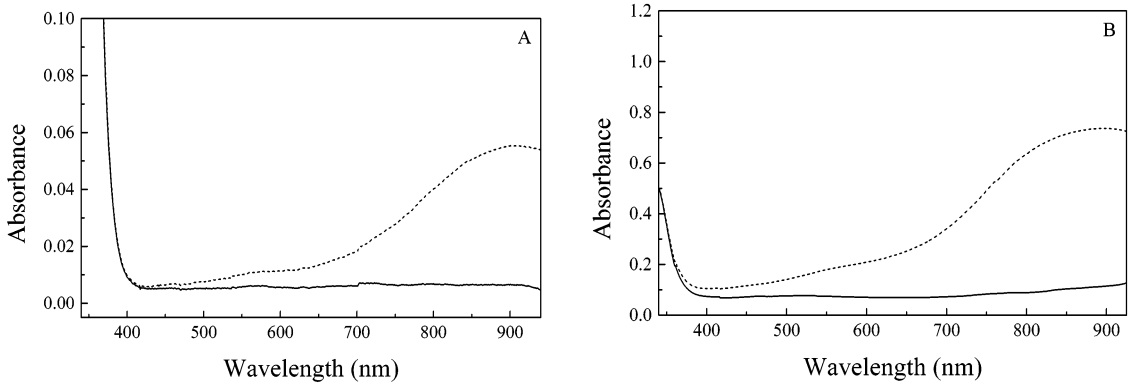

Figure 6. UV−vis spectra of (A) WO_3 and (B) WO_3/TiO_2 colloids. (—) Virgin state; (- -) after UV-light irradiation for 3 min.

which is consistent with the observation of larger particles by TEM (see Figure 3).

The fluorescence spectra of the colloids were collected because they can readily provide detailed information about the energy levels and the charge-transfer processes. Figure 5 gives the emission and excitation spectra of WO_3 (A) with and (B) without $H_2C_2O_4$, (C) TiO_2, and (D) WO_3/TiO_2 colloids. Since the difference in the wavenumber between the Raman peak of the solvent and the excitation light is almost constant, the Raman peak in the fluorescence spectra can thus be determined.[28] The shoulder or peak at ca. 365 nm in the emission spectra of Figure 5A, B, and D is suggested to be a Raman peak of the solvent when the excitation wavelength is at 315 nm. After deconvolution of the spectra in Figure 5A, B, and D, three peaks can be identified in both the emission (at ca. 385, 440, and 495 nm) and excitation spectra (at ca. 315, 345, and 385 nm). The sharp peak at ca. 385 nm in the excitation spectra of Figure 5A, B, and D results from the overlap of the Raman peak and the excitation of WO_3 at the emission wavelength of 440 nm. Two emission peaks at ca. 440 and 500 nm and one excitation peak at ca. 395 nm are identified in the fluorescence spectra of TiO_2 (Figure 5C). The peak at ca. 440 nm in the emission spectra of Figure 5C comes from the overlap of the Raman peaks of the solvent and the emission of TiO_2 at the excitation wavelength of 395 nm. It is found that the peak intensity of the emission spectra decreases after the addition of TiO_2 (Figure 5A and D) or after the removal of $H_2C_2O_4$ (Figure 5A and B).

Photochromism of the Colloids. Figure 6 is the UV−vis absorption spectra of (A) WO_3 and (B) WO_3/TiO_2 colloids. It is seen that both of them are almost transparent before UV-light irradiation. When WO_3/TiO_2 colloids are irradiated with UV light for 3 min, they turn deep blue, and a broad absorption

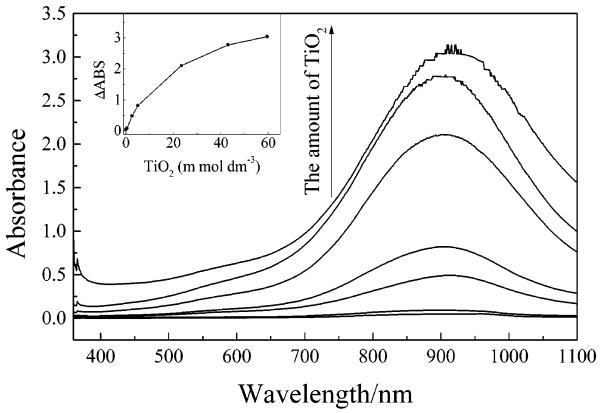

Figure 7. UV−vis spectra of the WO_3 colloids combined with TiO_2 nanoparticles at different concentrations; the virgin colloids are used as the references. The inset presents the dependence of ΔOD at 900 nm on the concentration of TiO_2.

peak at about 900 nm appears accordingly in the spectrum. However, the naked eye can hardly perceive the color change of the WO_3 colloids although the absorbance increases slightly after 3 min of UV-light irradiation (see Figure 6A). After a long period of irradiation (for example, 30 min) on WO_3 colloids, the blue color can be perceived visually. Since the photochromic response is accompanied by a change in absorbance, the magnitude of the difference in the absorbance (ΔOD) before and after the coloration is used to evaluate the coloration performance. According to Figure 6, ΔOD at 900 nm for WO_3/TiO_2 colloids (0.622) is about 12.7 times that of WO_3 colloids (0.049), whereas the molar ratio of TiO_2 to WO_3 is only about 1:40. Figure 7 shows the UV−vis absorption spectra of WO_3 colloids containing different amounts of TiO_2 by using the virgin state as the reference. The inset presents the dependence of the ΔOD at 900 nm on the concentration of TiO_2. It can be seen that the ΔOD increases with the increased concentration of TiO_2 and that the maximum amplitude can increase more than 50-fold.

The effects of $H_2C_2O_4$ on the photochromism of the colloids are also investigated. After the removal of $H_2C_2O_4$, the UV−vis absorption spectra of (A) WO_3 and (B) WO_3/TiO_2 colloids are recorded as shown in Figure 8. The inset of Figure 8B shows the dependence of the ΔOD at 900 nm on the concentration of TiO_2. Comparing Figures 6, 7, and 8, we found that ΔOD decreases obviously after the removal of $H_2C_2O_4$ by dialyzing against a H_2SO_4 solution with and without the presence of TiO_2. That is to say, both the existence of $H_2C_2O_4$ and the combination of TiO_2 can greatly improve the photochromic response of WO_3 colloids.

4. Discussion

The improvement of TiO_2 means that the quantity of photogenerated electrons that participate in the coloration process increases greatly in the composite system for the same amount of WO_3. Two reasons might account for this effect. One reason is that the total quantity of electrons originally generated in the system increases, which is a coincidence since TiO_2 is also a photoresponsive semiconductor. Another reason is that, even without the increase in the total quantity of electrons, the recombination process is suppressed and results in an improvement in the efficient utilization of photogenerated electrons. As discussed in Photochromic Mechanism (see below), the coloration is caused by the electrons trapped within the band gap of WO_3. To realize the second reason, therefore, the photogenerated electrons should transfer from TiO_2 to WO_3 in the composite system. The electron-transfer process is thus discussed below.

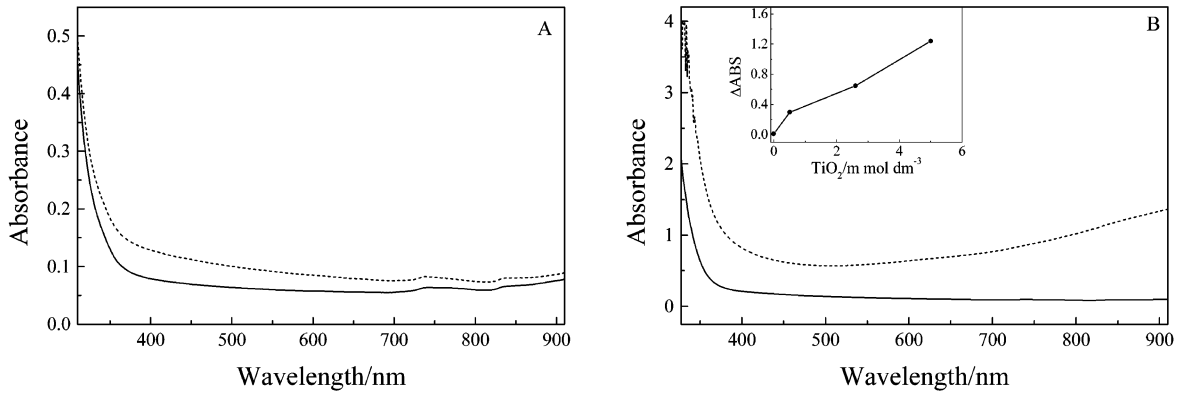

Figure 8. UV−vis spectra of (A) WO_3 and (B) WO_3/TiO_2 colloids after the removal of oxalic acid. (—) Virgin state; (- -) after UV-light irradiation for 30 min. The inset shows the dependence of ΔOD at 900 nm on the concentration of TiO_2.

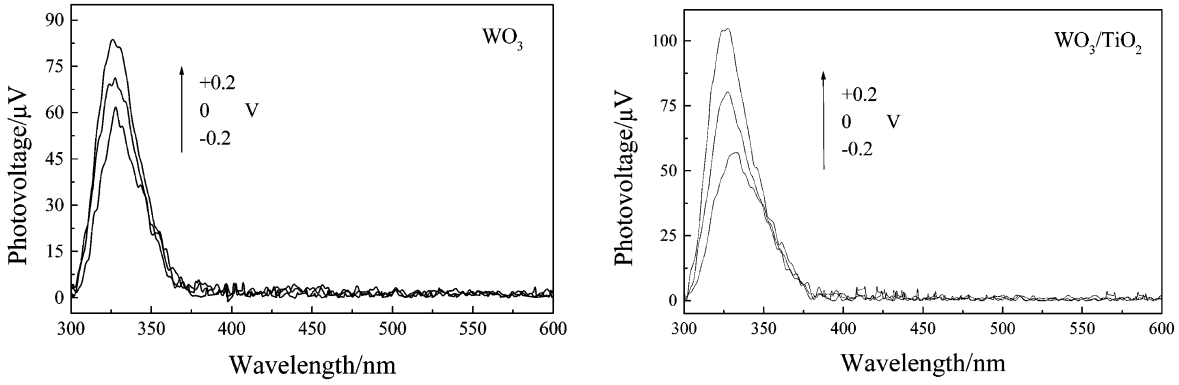

Figure 9. Electric field-induced SPS of WO_3 and WO_3/TiO_2 fine powders dried from the colloids.

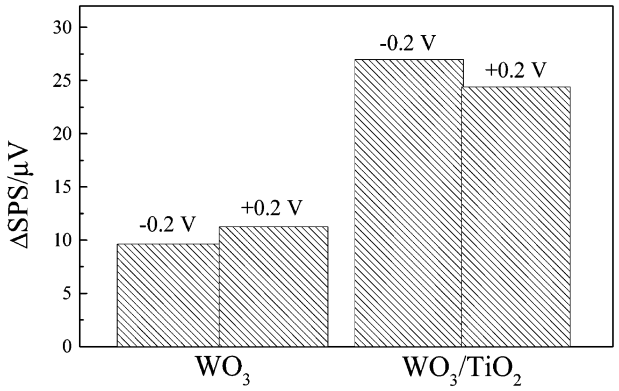

Figure 10. Scheme of the difference between the maximum in the SPS response of the unbiased samples and that of the ones biased with different voltages.

SPS Measurements and Determination of the Energy Levels. Since SPS is pertinent to the behavior of photogenerated electrons,[22,27] here it is used to investigate their transition or transfer process in the WO_3 or WO_3/TiO_2 system. Figure 9 gives the electric field-induced SPS of the WO_3 and WO_3/TiO_2 systems. The photovoltaic response at about 330 nm corresponds to the band-to-band transitions of the electrons. According to the SPS principle, the positive bias will increase the photovoltaic response whereas the negative bias will decrease it since either WO_3 or TiO_2 is a kind of n-type semiconductor, which is confirmed by Figure 9. Figure 10 is the scheme of the difference (ΔSPS) between the maximum photovoltaic response of the unbiased samples and the ones biased with a different voltage. It is found from Figure 10 that the ΔSPS of the WO_3/TiO_2 sample is larger than that of the WO_3 sample under the same negative or positive bias. This means that, in the composite system, more electrons will participate in the photovoltaic process under the positive bias and fewer electrons will take part in the process under the negative bias. Therefore, the electrons are able to transfer from TiO_2 to WO_3 according to the principle of SPS.[29] These results are consistent with the ones from fluorescence (Figure 5). The energy levels of the system are discussed next since they are closely related to the charge-transfer process.

It is known that the E_{fb} values of WO_3 and TiO_2 colloids are about 0.33 and -0.2 V (vs NHE), respectively, at pH 0.0.[6,7] Since the difference between the conduction-band minimum (E_{CB}) and E_{fb} is about 0.2 eV for both the WO_3 and TiO_2 semiconductors,[30] the E_{CB} values of WO_3 and TiO_2 are determined to be 0.13 and -0.40 V (vs NHE), respectively. The optical band gaps (E_g) of WO_3 and TiO_2 colloids can be derived as about 3.22 eV (385 nm) and 3.14 eV (395 nm), respectively, from a plot of $(\alpha h\nu)^{1/2}$ versus $h\nu$ based on the data shown in Figure 4, where α is the absorption coefficient.[18] Thus, the valence-band maxima (E_{VB}) of WO_3 and TiO_2 are 3.35 and 2.74 V (vs NHE), respectively. In addition, E_{VB} is approximately assumed to be the ground state in the emission spectra. The relative positions of the energy levels for the colloids can be determined according to the fluorescence spectra, as discussed above. Therefore, the schematic diagram of the energy levels of TiO_2 and WO_3 colloids can be illustrated as shown in Figure 11. It should be noted that the energy level here is the simplification of the energy band containing closely spaced ($\ll kT$) energy levels.

Photochromic Mechanism. When WO_3 colloids are irradiated with UV light ($h\nu \geq E_g$), the following reactions are expected to take place:[6-9]

$$WO_3 + h\nu \rightarrow WO_3(e_{CB}\cdots h_{VB}) \rightarrow WO_3(e_t + h_t) \quad (1)$$

$$WO_3(e_{CB}\cdots h_{VB}) + \text{scavenger} \rightarrow WO_3(e_t) + \text{products} \quad (2)$$

$$h^+ + e^- \rightarrow \text{heat} \quad (3)$$

where e and h refer to the photogenerated electron and hole, respectively. The electrons can be stimulated from the valence band to different energy levels of the conduction band (see Figure 11), and the holes are formed in the valence band at the same time. Then the holes may transfer to the surface and be scavenged there (eq 2). After being transmitted very quickly to the E_{CB} or lower energy levels within the forbidden gap through a nonradiative process (see Figure 11), the electrons may be trapped in these energy levels[9] or fall back to the valence band through a radiative (the extra energy is discharged in the form of fluorescence or phosphorescence) and/or nonradiative recombination of electron−hole pairs (eq 3).

The trapped electrons may be excited optically into the higher energy levels, which leads to a broad absorption in the red-IR region, as shown in Figures 6 and 7. Therefore, the colloids

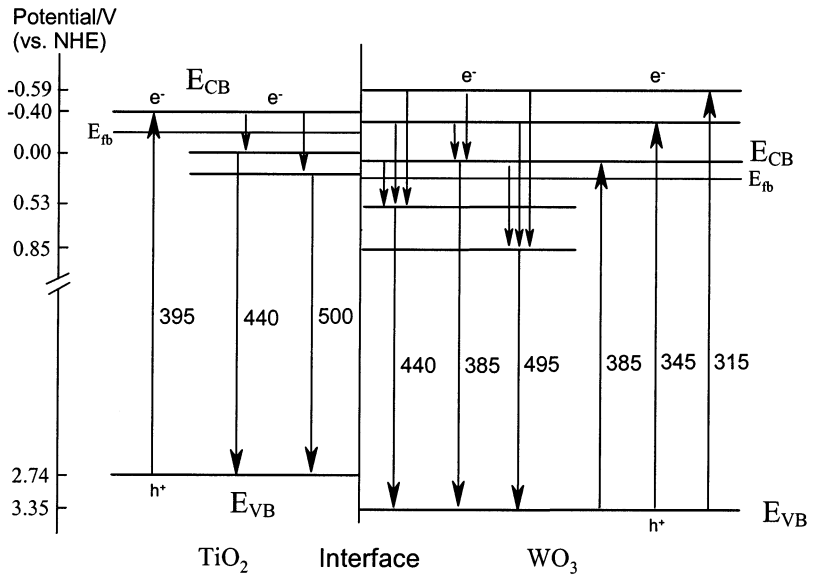

Figure 11. Schematic diagram of the energy levels of TiO_2 and WO_3 colloids.

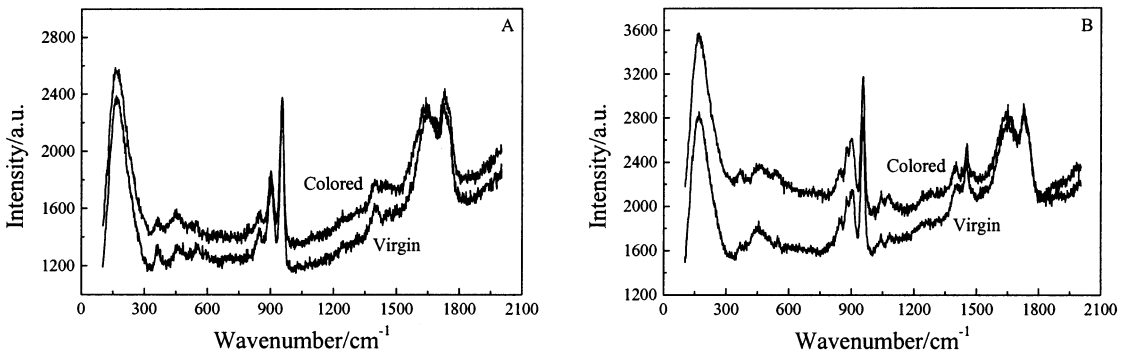

Figure 12. Raman spectra of (A) WO_3 and (B) WO_3/TiO_2 colloids before and after 10 min of UV-light irradiation.

can turn blue under UV-light irradiation. These trapped electrons are metastable since the blue color of the deaerated colloids fades gradually by exposure to air. However, their lifetime is relatively long in an inert atmosphere since the blue color can be retained for several days when the colored colloids are away from light. It is suggested that the broad absorption peak at ca. 900 nm in Figure 6 might result mainly from the transition of the trapped electrons from the energy level at 0.85 V (495 nm) to the one at −0.59 V (315 nm), of which the wavelength of the corresponding absorption light is ca. 861 nm. However, additional experiments are required to confirm this unequivocally.

The same absorption can also be obtained in WO_3 by the formation of hydrogen tungsten bronze.[19,22] To obviate this, Raman spectra of (A) WO_3 and (B) WO_3/TiO_2 colloids have been collected before and after UV-light irradiation, as shown in Figure 12. The spectra are almost identical before and after the coloration, which means that no hydrogen tungsten bronze is formed under UV-light irradiation.[15,16] It is known that the standard redox potential of hydrogen tungsten bronze is ca. −0.29 V (vs NHE).[31] However, this potential is insufficiently negative for the photogenerated electrons to reduce WO_3 to the hydrogen tungsten bronze[6] because almost all of the excited electrons will quickly fall to the lower energy levels ($\leq E_{CB}$) (at a rate on the order of picoseconds or femtoseconds) and the E_{CB} of WO_3 is ca. 0.13 V (vs NHE) in our system. The UV-light photochromism of TiO_2 in our system can also be obviated or ignored since its concentration is fairly low in our system. It is known that the characteristic absorption peak of TiO_2 sols is at ca. 560 nm.[5,25] However, a shoulder at ca. 560 nm appears in the absorption spectra of WO_3 colloids even without TiO_2 (see Figure 6A), indicating that there is no reduction of TiO_2 to contribute to the photochromism.

Enhancement Mechanism. It is known that the behavior of photogenerated carriers dictates the photochromism of WO_3. If photogenerated electrons and holes migrate in different directions, then the recombination will be suppressed and might result in improved photochromism of WO_3 colloids. When WO_3 is combined with TiO_2, the electrons and holes can be generated in either WO_3 or TiO_2 colloids when they are irradiated with UV light (see Figure 11). Some of the positive holes created in WO_3 can migrate to the valence band of TiO_2 particles because of a more positive potential of the valence band for WO_3. At the same time, the electrons at higher energy levels tend to transfer and/or fall back to lower energy levels. The more positive the energy-level potential is, the greater the electron-transfer efficiency. Therefore, most of the electrons created in WO_3 and TiO_2 particles will ultimately transfer to the energy level with the most positive potential (0.85 V) in WO_3, so the electrons and holes originally generated in either WO_3 or TiO_2 are separated efficiently, and their recombination is suppressed after the combining of TiO_2. As a result, more electrons will be trapped in the band gap of WO_3 and will contribute to the coloration process. At the same time, almost no reduction of TiO_2 takes place since the electrons tend to accumulate in WO_3, indicating that the photochromism of TiO_2 can be excluded in this system. Although the recombination process is suppressed, only a slight change in the emission intensity of WO_3 is observed after the TiO_2 combination (Figure 5A and D). This means that the quantity of electrons participating in the recombination process hardly changes in the composite system. This is reasonable since the total quantity of electrons originally generated in the system upon UV-light irradiation increases after the combination with TiO_2 because TiO_2 is also a photoresponsive semiconductor.

As discussed above, the TiO_2 combination can improve the photochromism of WO_3 because both the E_{CB} and E_{VB} values of TiO_2 are more negative than those of WO_3. This point is further supported by the combination of WO_3 with another photoresponsive semiconductor with more-positive E_{CB} and E_{VB} values (i.e., SnO_2). There is almost no improvement in photochromism observed for the WO_3/SnO_2 system. Since the E_{CB} and E_{VB} values of SnO_2 are more positive than those of WO_3,[2] photogenerated electrons will accumulate in the conduction band of SnO_2, and the holes will accumulate in the valence band of WO_3. Therefore, most of the photogenerated electrons cannot participate in the coloration process although the recombination process can also be suppressed. This also indicates that the photochromism is caused by the electrons trapped within the band gap of WO_3, so SnO_2 can hardly improve the photochromism of WO_3.

After the removal of $H_2C_2O_4$, the peak intensity of the emission spectra of WO_3 decreases greatly (see Figure 5A and B). This indicates that the recombination process of the photogenerated charge carriers is suppressed greatly by $H_2C_2O_4$. This is reasonable since $H_2C_2O_4$ can act as an efficient scavenger of the holes because it is reducible and can be oxidized by photogenerated holes.[32,33] Therefore, the photochromism of WO_3 colloids can be improved by $H_2C_2O_4$.

5. Conclusions

The photochromism of WO_3 colloids can be improved greatly by the combination of TiO_2. First, the total quantity of electrons originally generated in the system increases after the combination since TiO_2 is also a photoresponsive semiconductor. More importantly, most electrons will accumulate in WO_3, resulting in the efficient suppression of the recombination process of electrons and holes after the combination. Therefore, more photogenerated electrons will contribute to the coloration process in the composite system and will lead to improved photochromism.

Acknowledgment. This work is sponsored by the National Research Fund for Fundamental Key Projects no. 973 (G19990330), the National Science Foundation of China, and the Chinese Academy of Sciences.

References and Notes

(1) Henglein, A. *Chem. Rev.* **1989**, *89*, 1861.
(2) Hagfeldt, A.; Grätzel, M. *Chem. Rev.* **1995**, *95*, 49.
(3) Leland, J. K.; Bard, A. J. *J. Phys. Chem.* **1987**, *91*, 5083.
(4) Li, S. T.; Germanenko, I. N.; Ei-Shall, M. S. *J. Phys. Chem. B* **1998**, *102*, 7319.
(5) Kormann, C.; Bahnemann, D. W.; Hoffman, M. R. *J. Phys. Chem.* **1988**, *92*, 5196.
(6) Nenadović, M. T.; Rajh, T.; Mićić, O. I.; Nozik, A. J. *J. Phys. Chem.* **1984**, *88*, 5827.
(7) Dimitrijević, N. M.; Savić, D.; Mićić, O. I.; Nozik, A. J. *J. Phys. Chem.* **1984**, *88*, 4278.
(8) Kamat, P. V. *Chem. Rev.* **1993**, *93*, 267.
(9) Bedja, I.; Hotchandani, S.; Kamat, P. V. *J. Phys. Chem*. **1993**, *97*, 11064.
(10) Sun, M.; Xu, N.; Cao, Y. W.; Yao, J. N.; Wang, E. G. *J. Mater. Res.* **2000**, *15*, 927.
(11) Xu, N.; Sun, M.; Cao, Y. W.; Yao, J. N.; Wang, E. G. *Appl. Surf. Sci.* **2000**, *157*, 81.
(12) Bechinger, C.; Oefinger, G.; Herminghaus, S.; Leiderer, P. *J. Appl. Phys.* **1993**, *74*, 4527.
(13) Bechinger, C.; Wirth, E.; Leiderer, P. *Appl. Phys. Lett.* **1996**, *68*, 2834.
(14) Yao, J. N.; Loo, B. H.; Hashimoto, K.; Fujishima, A. *Ber. Bunsen-Ges. Phys. Chem.* **1991**, *95*, 554.
(15) Yang, Y. A.; Cao, Y. W.; Chen, P.; Loo, B. H.; Yao, J. N. *J. Phys. Chem. Solids* **1998**, *59*, 1667.
(16) Yang, Y. A.; Yao, J. N. *J. Phys. Chem. Solids* **2000**, *61*, 647.
(17) Yang, Y. A.; Ma, Y.; Yao, J. N.; Loo, B. H. *J. Non-Cryst. Solids* **2000**, *272*, 71.
(18) Deb, S. K. *Philos. Mag.* **1973**, *27*, 801.
(19) Faughnan, B. W.; Crandall, R. S.; Hyman, P. M. *RCA Rev.* **1975**, *36*, 177.
(20) Mo, Y.-G.; Dillon, R. O.; Snyder, P. G. *J. Vac. Sci. Technol., A* **1999**, *17*, 2933.
(21) He, T.; Ma, Y.; Cao, Y. A.; Yang, W. S.; Yao, J. N. *J. Electroanal. Chem.* **2001**, *514*, 129.
(22) He, T.; Ma, Y.; Cao, Y. A.; Yang, W. S.; Yao, J. N. *Phys. Chem. Chem. Phys.* **2002**, *4*, 1637.
(23) Ohtani, B.; Atsumi, T.; Nishimoto, S.; Kagiya, T. *Chem. Lett.* **1988**, 295.
(24) Tennakone, K.; Heperuma, O. A.; Bandara, J. M. S.; Kiridena, W. C. B. *Semicond. Sci. Technol.* **1992**, *7*, 423.
(25) Guan, Z. S.; Ma, Y.; Cao, Y. A.; Ji, X. H.; Yao, J. N. *Acta Phys.-Chim. Sin.* **2000**, *16*, 5.
(26) Wang, B. H.; Wang, D. J.; Cao, Y. W.; Chai, X. D.; Geng, X. H.; Li, T. J. *Thin Solid Films* **1996**, *284/285*, 588.
(27) He, T.; Ma, Y.; Cao, Y. A.; Jiang, P.; Zhang, X. T.; Yang, W. S.; Yao, J. N. *Langmuir* **2001**, *17*, 8024.
(28) Parker, C. A. *Analyst (Cambridge, U.K.)* **1959**, *84*, 446.
(29) Wang, D. J.; Liu, W.; Xiao, L. Z.; Li, T. J. *Huaxue Tongbao* **1989**, *10*, 32.
(30) Morrison, S. R. *Electrochemistry at Semiconductor and Oxidized Metal Electrodes*; Plenum Press: New York, 1980; Chapter 2.
(31) Hitchman, M. L. *J. Electroanal. Chem.* **1977**, *85*, 135.
(32) Kulas, J.; Roušar, I.; Krýsa, J.; Jirkovský, J. *J. Appl. Electrochem.* **1998**, *28*, 843.
(33) Krýsa, J.; Bouzek, K.; Stollberg, Ch. *J. Appl. Electrochem.* **2000**, *30*, 1033.